Supplementary Material S1. Biojet fuel Production and Combustion

The biojet fuel production comprises eight stages:

1. **Resin Preheating.** Once the resin or pine resin is collected, it is taken to the distillation factory. There, it is preheated up to 450 K. The pressure, temperature and mass flow conditions of this stream are 1 atm, 293 K and 1000 kg/h respectively. For the increase in temperature, it has been assumed that it would be by heat transfer from the water vapour that is produced in a natural gas boiler. The heat transfer efficiency of the exchanger is 90%. This performance is applied to all processes where heat is required.

   According to the simulation in ASPEN, to obtain 1000 kg of resin or preheated resin, 86.854 kWh is necessary, but applied the heat exchanger performance the consumption amounts 96.504 kWh (see Table S1.1).

Table S1.1. Inventory of Resin Preheating Process

Materials and Fuels Inputs	Resin, Pinus Pinaster, ES	1000	kg
Electricity and Heat Inputs	Process steam from natural gas, heat plant, consumption mix, at plant, MJ ES S	96.50	kWh
Outputs	Preheated Resin, ES	1000	kg

2. **Resin Filtering.** Resin impurities have to been removed prior distillation. No energy consumption has been considered for this process. Only solid impurities such as splinters or pine spikes must be removed before distillation. They account around 2 % of the preheated resin. From a conservative point of view, they are considered residues. Nevertheless, since pitch or tar could be obtained by their slow combustion, they could have an economic value in the market. This would slightly benefit the environmental performance and the price of the obtained biojet fuel. All the environmental impacts are allocated to resin, as it can be seen in Table S1.2.

Table S1.2. Inventory of Resin Filtering Process

				Allocation
Materials and Fuels Inputs	Preheated Resin, ES	1000	kg	
Outputs	Pure Resin, ES	980	kg	100 %
	Solid Impurities	20	kg	0 %

3. **Resin Distillation.** Distillation is a process that takes advantage of the difference in boiling points that the components of a mixture may have for their separation. The further the boiling points of the substances are, the more effective the distillation.

   The reference temperature taken for the distillation is 453 K, which is a temperature that is slightly above the boiling point of the α-pinene and β-pinene compounds. These are the main compounds of turpentine.

   The amount obtained from the distillate products and residues is shown in Table S1.3. Mass allocation of environmental loads between products were taken into account. The distillate residue is considered to go to wastewater treatment.

   On the one hand, distillation requires an input of heat energy to heat the mixture to operating temperature. On the other hand, cooling energy is necessary to condense the lighter fraction of the distillation.

   For calorific consumption, the same criteria are applied as in resin preheating. In the case of refrigeration energy, it is considered that the refrigeration is carried out by a refrigeration circuit that has an EER (Energy Eficiency Ratio) of 3.5. Table S1.3 also shows the inputs of both energy and matter necessary to obtain the different outputs of the process.

Table S1.3. Inventory of Resin Distillation Process

Materials and Fuels Inputs	Pure Resin, ES	1000	kg
Electriciy and Heat Inputs	Process steam from natural gas, heat plant, consumption mix, at plant, MJ ES S	148.51	kWh
	Electricity, medium voltage {ES}| market for | APOS, U	1.0017	kWh
Outputs	Turpentine, ES	132.12	kg
	Rosin, ES	866.16	kg
Residues and emissions	Wastewater, average {Europe without Switzerland}| market for wastewater, average | APOS, U	1.72	dm^3

4. **Turpentine Decantation.** When leaving the distillation, the turpentine incorporates a percentage of water that can be separated by decantation thanks to the insolubility of turpentine with water.

   In order to carry out this process, the turpentine is cooled a few degrees below its boiling point. The purified turpentine is extracted from the mixture in the form of a liquid while the water remains in the gaseous state.

Once this process is finished, the excess water from the process is cooled so that it can be disposed of as waste and sent to wastewater treatment.

In both processes, the required energy is for refrigeration (see Table S1.4).

Table S1.4. Inventory of Turpentine Decantation Process

Materials and Fuels Inputs	Turpentine, ES	132.12	kg
Electriciy and Heat Inputs	Electricity, medium voltage {ES}| market for | APOS, U	2.6017	kWh
	Electricity, medium voltage {ES}| market for | APOS, U	1.1580	kWh
Outputs	Purified turpentine, ES	126.88	kg
Residues and emissions	Wastewater, average {Europe without Switzerland}| market for wastewater, average | APOS, U	5.24	dm^3

5. **Compression and Preheating of purified turpentine.** For the conversion of purified turpentine into biojet fuel, the purified turpentine has to meet a series of requirements for the conversion to be 100%. That is, it must enter the reactor at 11 atm and 473 K. At the outlet of the decanter, the current is at 423 K and 1 atm of pressure. For this reason, the current must first go through a compression and preheating process. Compression occurs isentropically so as not to alter the entropy of the purified turpentine. The inventory of this process is collected in Table S1.4.

Table S1.5. Inventory of Compression and Preheating of purified turpentine processes.

Materials and Fuels Inputs	Purified turpentine, ES	126.88	kg
Electriciy and Heat Inputs	Electricity, medium voltage {ES}| market for | APOS, U	0.077	kWh
	Process steam from natural gas, heat plant, consumption mix, at plant, MJ ES S	4.49	kWh
Outputs	Compressed and preheated purified turpentine	126.88	kg

6. **Compressed hydrogen conditioning.** Hydrogen feed is assumed under high pressure conditions (200-400 atm, 20-40 MPa). To meet the same pressure and temperature conditions than the turpentine, it undergoes an isentropic expansion and an increase in temperature. It has been considered that the energy generated in the expansion is not reused in the process, since a generator would be needed

to transform this energy into electricity and this is not feasible. With all these requirements, the inventory of this process is collected in Table S1.6.

Table S1.6. Inventory of Compress hydrogen conditioning.

Materials and Fuels Inputs	Hydrogen, compressed| market for | APOS, U	2.1	kg
Electricity and Heat Inputs	Process steam from natural gas, heat plant, consumption mix, at plant, MJ ES S	1.64	kWh
Outputs	Conditioned hydrogen	2.1	kg

However, the compressed hydrogen production process was not included in Ecoinvent database, so the compression process was simulated in ASPEN and the data were modified in an existing process in Agri-footprint database (Hydrogen gas, from membrane technology, at plant/RER Mass).

The inventory data for this process is included in Table S1.7.

Table S1.7. Inventory of compressed hydrogen production.

Materials and Fuels Inputs	Transport, freight, lorry, unspecified {GLO}| market for | APOS, U	0.00567	tkm
	Transport, freight, light commercial vehicle {GLO}| market for | APOS, U	0.00018	tkm
	Hydrogen gas, from membrane technology, at plant/RER Mass	1	kg
	Transport, freight train {CN}| market for | APOS, U	0.00104	tkm
	Transport, freight train {US}| market for | APOS, U	0.00146	tkm
	Transport, freight train {RoW}| market for | APOS, U	0.0019	tkm
Electricity and Heat Inputs	Electricity, medium voltage {ES}| market for | APOS, U	5.9	kWh
	Electricity, medium voltage {ES}| market for | APOS, U	1.68	kWh
Outputs	Hydrogen,compressed| market for | APOS, U	1	kg

7. ***Purified turpentine hydrogenation*.** Turpentine need to be hydrogenated to meet minimums established by ASTM D7566 for use as aviation fuel (Bolonio et al., 2018). This process has been simulated by a stoichiometric reactor (RStoic) in Aspen Plus. The inlet to this reactor has two feeds, one of purified turpentine and the other of hydrogen. The hydrogenation of purified turpentine occurs between 423-473 K at a pressure of 1-11 atm.

Reactor was operated at 11 atm (1.1 MPa) and 473 K in the presence of 1% Pt / Al_2O_3, which acts as a catalyst. The hydrogenation reaction yield is 95%. The inventory of this process is collected in Table S1.8.

Table S1.8. Inventory of purified turpentine hydrogenation process.

Materials and Fuels Inputs	Conditioned hydrogen	2.1	kg
	Compressed and preheated purified turpentine	126.88	kg
Outputs	Biojet fuel, hydrogenation, ES	128.98	kg

8. **Biojet fuel conditioning.** Once out of the reactor, the biojet fuel is at a very high temperature and pressure to be able to be transported to the point of consumption. Therefore, it undergoes an expansion process followed by a temperature drop. The desired temperature and pressure conditions are 1 atm and 298 K. As in the expansion of hydrogen, that energy will not be taken into account in the process. The inventory data for this process are collected in Table S1.9.

Table S1.9. Inventory of Biojet fuel conditioning process.

Materials and Fuels Inputs	Bioje fuel, hydrogenation, ES	128.98	kg
Heat and Energy Inputs	Electricity, medium voltage {ES}| market for | APOS, U	3.8074	kWh
Outputs	Biojet fuel, normal conditions, ES	128.98	kg

Biojet Fuel Combustion. Emissions inventory is adapted from data collected in a Boeing 737-400 by the European Environmental Agency (European Environment Agency, 2019) and are shown in Table S1.10.

Table S1.10. Inventory of the biojet fuel combustion process.

Materials and Fuels Inputs	Biojet fuel, normal conditions, ES	3140.69	kg
Residues and emissions	Carbon dioxide, biogenic	9893.16	kg
	Nitrogen oxides	48.41	kg
	Water	3863.04	kg
	Carbon monoxide, biogenic	6.1	kg
	Particulates, < 10 μm (mobile)	0.3139	kg
	Hydrocarbons, unspecified	0.89	kg
Outputs	Biojet fuel, combustión, gas engine, plane, ES	3140.69	kg

Supplementary Material S2. Transports

As stated in section 2.1.2., three transports have been considered. The two firsts transports are going to be described in more detail in this section S2.

1. *Resin transport from the pine forest to the distillation factory***.** The forests with largest areas were chosen and the number of pine forest selected from each province were linked to their resin production. Therefore, for every 1,000 t of resin produced per locality, a pine forest is assigned. The locations of the pine forests are represented by a tree in Figure S2.1.

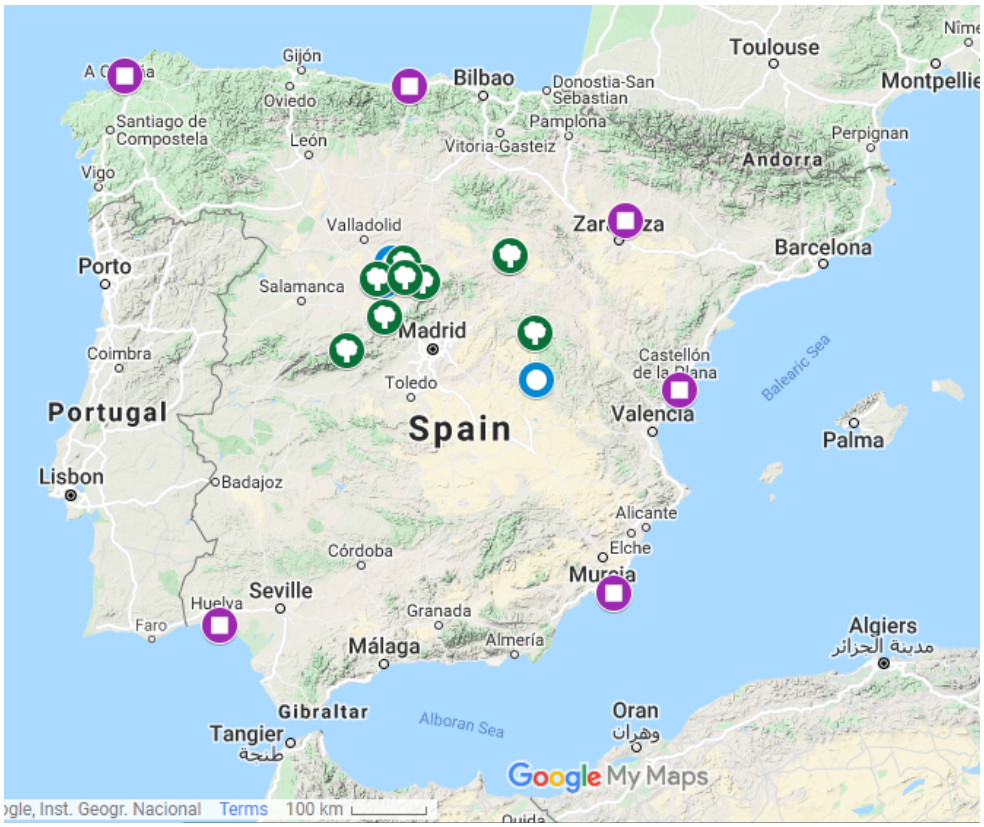

Figure S2.1. Location of pine forests (represented by a tree), resin distilleries (represented by a circle) and biorefineries (represented by a square).

Resin distillate factories are only reduced to 7 in Spain. Five of them are in Segovia, one in Soria and the last in Cuenca (represented by circles in Figure S2.1).

To obtain the average distance between a factory and a pine forest in Spain, all the distances between the factories and the chosen pine forests have been calculated. The proximity between the factory and the pine forest has not been taken into account since it has been considered that the resin will be sold to the best buyer.

Oversized transport has been preferred due to the shortage of still factories. With these values, an average value has been calculated, which is indicated at the end of Table S2.1.

Table S2.1. Distances between distilleries and pine forests.

Distillery	Pine Forest	Location	Distance (km)
Industrial Resinera Valcán S. A. (Cuenca)	Cabeza Carrascosa	Cuenca	29
	Común Grande de las Pegueras	Segovia	324
	Pinar Viejo	Segovia	319
	El Rebollo	Segovia	304
	El Pinar Aguilafuente	Segovia	311
	Pinar de Maniel y agregados	Segovia	263
	Pinar y Sierra	Ávila	302
	Pinar de Almazán	Soria	247
Resinas Naturales (Soria)	Cabeza Carrascosa	Cuenca	212
	Común Grande de las Pegueras	Segovia	188
	Pinar Viejo	Segovia	201
	El Rebollo	Segovia	147
	El Pinar Aguilafuente	Segovia	171
	Pinar de Maniel y agregados	Segovia	217
	Pinar y Sierra	Ávila	325
	Pinar de Almazán	Soria	10
Resinas Naturales (Segovia)	Cabeza Carrascosa	Cuenca	189
	Común Grande de las Pegueras	Segovia	12
	Pinar Viejo	Segovia	25
	El Rebollo	Segovia	46
	El Pinar Aguilafuente	Segovia	33
	Pinar de Maniel y agregados	Segovia	81
	Pinar y Sierra	Ávila	199
	Pinar de Almazán	Soria	189
Eleuterio Criado Gómez (Segovia)	Cabeza Carrascosa	Cuenca	331
	Común Grande de las Pegueras	Segovia	14
	Pinar Viejo	Segovia	50
	El Rebollo	Segovia	26
	El Pinar Aguilafuente	Segovia	8
	Pinar de Maniel y agregados	Segovia	68
	Pinar y Sierra	Ávila	205
	Pinar de Almazán	Soria	171
Resinas Alfonso Criado (Segovia)	Cabeza Carrascosa	Cuenca	335
	Común Grande de las Pegueras	Segovia	9
	Pinar Viejo	Segovia	41
	El Rebollo	Segovia	43
	El Pinar Aguilafuente	Segovia	17
	Pinar de Maniel y agregados	Segovia	71

	Pinar y Sierra	Ávila	202
	Pinar de Almazán	Soria	191
Luresa Resinas (Segovia)	Cabeza Carrascosa	Cuenca	335
	Común Grande de las Pegueras	Segovia	43
	Pinar Viejo	Segovia	7
	El Rebollo	Segovia	70
	El Pinar Aguilafuente	Segovia	44
	Pinar de Maniel y agregados	Segovia	48
	Pinar y Sierra	Ávila	170
	Pinar de Almazán	Soria	217
Resina Navas de Oro (Segovia)	Cabeza Carrascosa	Cuenca	322
	Común Grande de las Pegueras	Segovia	36
	Pinar Viejo	Segovia	14
	El Rebollo	Segovia	62
	El Pinar Aguilafuente	Segovia	36
	Pinar de Maniel y agregados	Segovia	48
	Pinar y Sierra	Ávila	175
	Pinar de Almazán	Soria	209
		Average Distance	**142.2**

2. *Purified turpentine transport from the distillation factory to the biorefinery*. To estimate the mean distance between distillate factories and biorefineries, the same procedure and considerations have been carried out. Biorefineries that could have potential for the production of biojet fuel have been georeferenced, taking into account that their production processes include hydrogenation (represented by squares in Figure S2.1). The distances from all these biorefineries to the distillate factories have been calculated, obtaining the values shown in Table S2.2.

Distillery	**Biorefinery**	**Location**	**Distance (km)**
Industrial Resinera Valcán S. A. (Cuenca)	Undesa	Zaragoza	200
	Masol Iberia Biofuel	Castellón	364
	Masol Iberia Biofuel	Cartagena	616
	Masol Iberia Biofuel	Ferrol	656
	Sniace	Cantabria	353
	Bio-oils	Huelva	817
Resinas Naturales (Soria)	Undesa	Zaragoza	379
	Masol Iberia Biofuel	Castellón	576
	Masol Iberia Biofuel	Cartagena	613
	Masol Iberia Biofuel	Ferrol	513
	Sniace	Cantabria	283
	Bio-oils	Huelva	735

Resinas Naturales (Segovia)	Undesa	Zaragoza	327
	Masol Iberia Biofuel	Castellón	266
	Masol Iberia Biofuel	Cartagena	362
	Masol Iberia Biofuel	Ferrol	781
	Sniace	Cantabria	557
	Bio-oils	Huelva	669
		Average Distance	**503.7**

Supplementary Material S3. Payload vs. range analysis

The payload is the useful weight that the airplane can carry generating an income for the airline, usually the passengers and the cargo, and taking as fixed the remaining airplane weights. The range is considered the maximum distance that an airplane can cover at constant height and speed, without the influence of external forces. The payload vs. range graphics relate the distance that an airplane can cover with the payload and it usually has the form of Fig. S3.1, with three different zones: AB, BC and CD.

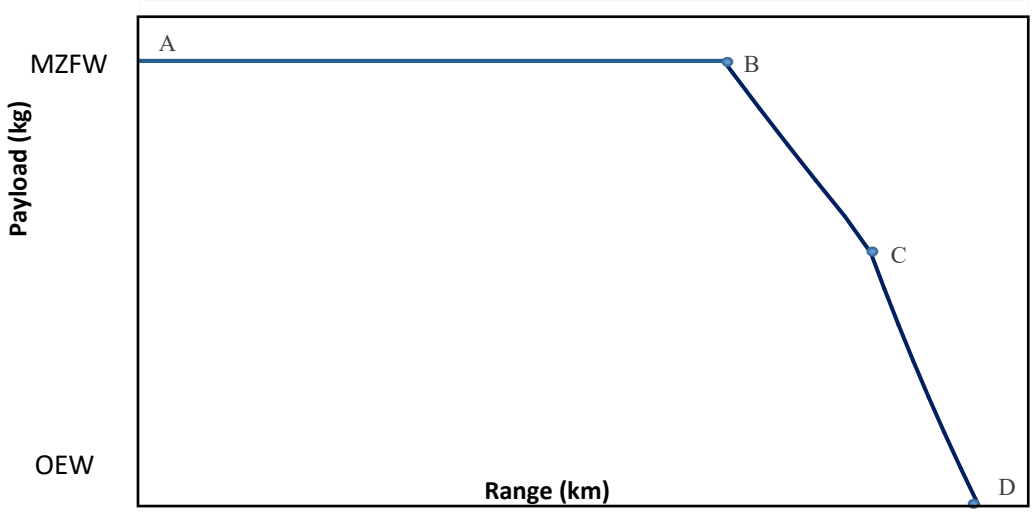

Fig. S3.1. Generic "payload vs range" graphic (*MZFW* – Max Zero Fuel Weight; *OEW:* Operational Empty Weight).

- In point A, the airplane has the tank empty and the maximum payload (Max Zero Fuel Weight: MZFW). This maximum payload is limited by the structural airplane design and can be increased only by the manufacturer.

- In segment AB, with a maximum payload, the fuel tank is filled until the maximum design weight of the airplane, W_0.
- In point B, the maximum flying weight of the airplane is reached. This point represents the maximum fuel load and the maximum range for a maximum payload.
- In segment BC, the payload decreases and the fuel weight increases until reaching the maximum airplane weight, W_0. At increasing the fuel weight, the range increases. Point C represents the fuel tank full. With this amount of fuel, the airplane has the most reasonable payload with the best economic benefit.
- Segment CD represents the increasing of range but with reduction of payload at maximum fuel weight. The points of this segment are not economically viable, since for a small range increase, great payload reductions are needed. Moreover, the airplane is consuming more energy than necessary, and thus, in this segment, the fuel amount is reduced.
- Point D represents the maximum range that the airplane can reach, with the fuel tank full and without any payload (Operational Empty Weight, OEW).

The payload vs. range calculations were carried out using three approaches: the Breguet equation[62], the Raymer model[63], and the PIANO software[64]

A) Breguet equation

The Breguet equation (Eq. 1)[59] estimates the range supposing that the airplane is in straight and level flight for the whole flight, without turbulences and with the fuel tank full at the beginning of the flight.

$$Range = \frac{V\left(\frac{L}{D}\right)}{g \cdot sfc} ln\left(\frac{W_i}{W_f}\right) \quad \text{Eq. 1}$$

where: V is the flight speed; (L/D) is the lift/drag ratio of each aircraft (a characteristic that depends of the airplane type); g is the gravitational constant (9.81 m/s^2); sfc is the specific fuel consumption (mg/(N·s)); W_i ($W_{empty} + W_{payload} + W_{fuel}$); and W_f ($W_{empty} + W_{payload}$) are the initial and final airplane weights, respectively.

The *L/D* ratio indicates the aerodynamic performance of the aircraft, relating two aerodynamic forces: lift and drag. The value of these forces depends on the shape of the airplane, its size, its speed and the air conditions. It has a high value if the shape produces a lot of push or little drag. When the aircraft is flying at a constant speed, the lift force is equal to the weight, so with a high *L/D,* the loaded payload can be higher. The recoil force (drag) will also be equal to the advance force (lift), therefore, if the recoil force is small, so will the advance force be. The advance force is produced by burning fuel, so a low recoil would indicate a low fuel consumption, which allows a longer flight time. A high *L/D* ratio would indicate that the aircraft is optimal for freight or long-distance routes. It is calculated by equation 2, dividing the lift coefficient (C_l) and the drag coefficient (C_d). Both can be measured in wind tunnels or mathematically calculated for simple shapes[63].

$$\frac{L}{D} = \frac{C_l}{C_d} \qquad \text{Eq. 2}$$

The specific fuel consumption *sfc* is usually proportional to the lower heating value of the biofuel.

The payload vs. range was calculated up to the maximum volumetric capacity of the fuel tank for an Airbus A300 600R, whose characteristics are included in Table S3.1[65].

Table S3.1. Data for the airplane Airbus 300-600R.

W_0 (kg)	170.500
W_{empty} (kg)	89.813
$W_{payload}$ (kg)	40.500
V_{tank} (m^3)	68.15
L/D	16.37

The density of the blends ρ was calculated from the densities of the hydroturpentine and Jet A1 following equation 3:

$$\frac{1}{\rho} = \sum_i \frac{Y_i}{\rho_i}$$

Eq. 3

where ρ is the blend density, Y_i is the mass fraction of each component and ρ_i is the density of each component.

B) Raymer model

The airplane range has been calculated (equation 4) following the Raymer model[60]:

$$Range = \frac{167.64\ \eta\ L}{sfc_{fuel}\ D} ln\left[\frac{0.975 W_0}{W_0 - W_{fuel}}\right]$$

Eq. 4

where *Range* is expressed in meters, η is the turbine yield, sfc_{fuel} is the specific fuel consumption in kilograms per hour per Joule (kg/(J·h)), *L/D* is the lift to drag ratio, W_o is the maximum design weight of the airplane (kg), and W_{fuel} is the fuel weight (kg). The model accuracy is higher than the Breguet equation, allowing to change the flight conditions, the height and the flying time.

C) PIANO software.

PIANO is a software created for the analysis of commercial airplanes, developed by the Lissys Company[62]. It can be used for preliminary design, yield studies and environmental emissions, and it is employed by companies such as Boeing or Rolls-Royce. In this work, the free version PIANO-X of the PIANO-5 version has been used, with the handicap that it can be applied only to some airplanes, and this is the reason for choosing the Airbus A300 600R in this work. The accuracy of the results is also higher than the Breguet equation, since it takes into account some parameters which in the Breguet model remain constant, like the airplane height. Moreover, this software accounts for a different fuel consumption during the take-off, the steady flight and the landing. This software also reports the detailed emissions during the different stages of the flight.

The payload vs. range results of the PIANO and Raymer models are quite similar, and definitely more accurate than the Breguet equation results.

Table 3 shows the fuel parameters used for the payload vs. range calculations in the three models. The density of hydroturpentine (859.7 kg/m^3) is much higher than that of Jet A1 (783.6 kg/m^3), and the *LHV* of both fuels is practically the same. Thus, the range for an airplane fuelled with pure hydroturpentine is significantly higher than for Jet A1. For the blends of hydroturpentine and Jet A1, the range is slightly increased with the amount of hydroturpentine due to its higher density. The energy density (ED) in a volumetric basis is quite similar for both fuels, somewhat higher for hydroturpentine.

The Breguet equation is the simplest flight model and assumes that the biofuel is burned as efficiently as Jet A1, and that no structural changes to the plane are necessary to accommodate the new fuels. Due to all of these assumptions, this model normally overestimates the range and it is intended to be used as a method of comparison between the fuels rather than an accurate depiction of the range of an operating aircraft. To simplify the assessment, the equation was used up to the volumetric limit of the fuel. The flat portion of the graph at approximately 40.000 kg payload is the range at the maximum payload capacity of the aircraft. The range at maximum payload increases as more fuel is added. The first change in payload corresponds to the point at which the maximum structural weight of the airframe W_0 is reached, after which, any additional fuel added would lead to an increase in range, at the expense of reducing payload by removal of cargo or passengers in order to accommodate the weight of the additional fuel.

Fig. S3.2 show the graphics of payload vs. range for pure hydroturpentine, using the three models of this work. As it was expected, the Breguet equation overestimates the range, with the Raymer and PIANO models showing very similar results. although the PIANO result is more conservative. Hydroturpentine can reach a higher range, up to 10,000 km in the Raymer model, due to its higher density. However, as it is highly improbable that an airplane would be fuelled with pure biofuel in the near future, graphics of payload vs. range for blends of hydroturpentine with Jet A1 have been represented in Fig. S3.3, using in this case only the Raymer model. This model was chosen because its accuracy is almost equal to that of PIANO but it allows to use any airplane, which is not possible in the free PIANO-X version.

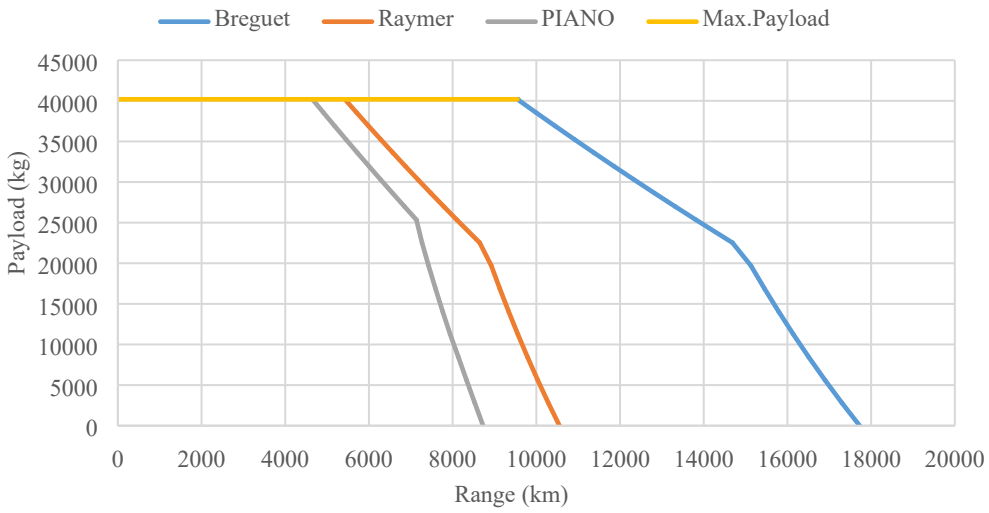

Fig. S3.2. Payload vs. range for hydroturpentine with the three models.

An airplane fuelled with blends of hydroturpentine and Jet A1 is expected to suffer a slight decrease in its flying range, since its energy for a given volume of fuel is a little lower. The optimal flying point for the blends will be 25,000 kg payload with a range of 8,250 km. Fig. S3.3 shows that the performance of the blends is practically the same as that of Jet A1, making this biofuel an excellent drop-in alternative. Moreover, from a payload of 20,000 kg and a range of 8,250 km, hydroturpentine performs better than Jet A1.

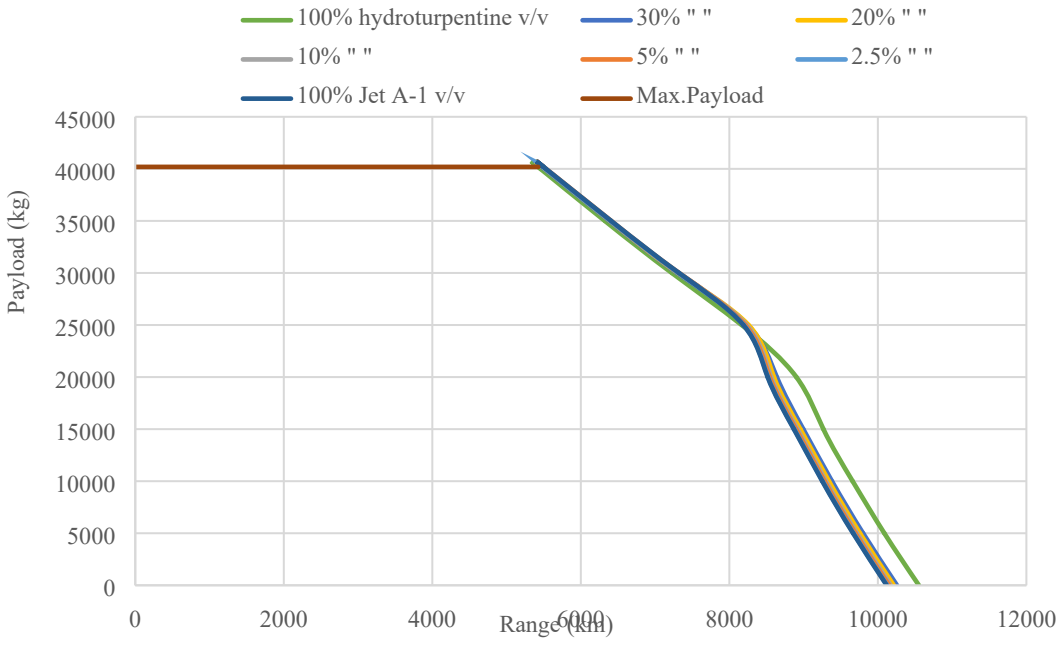

Fig. S3.3. Graphic of payload vs range for blends of hydroturpentine and Jet A1 (Raymer model).